Construction of Response Models for Color Gradation Skewed Distribution Parameters Extracted from Digital Wheat Canopy Images in Response to Cold-Spell Effects

Jibo Zhang,[a,b] Hongwei Zhou,[c,*] Chuanxiang Yi,[c] Pei Zhang,[d] Haijun Huan,[e] Feifei Xu,[c] Qi Chen,[f] Qiqing Shan,[f] Ye Sheng,[c] and Qin Mei [c]

This study examined the response of color information in digital wheat canopy images from Shandong Province, China, to meteorological indicators during extreme cold spells. Analysis revealed that low-temperature stress altered pixel color and grayscale values, with shifts captured by skewness and kurtosis parameters of color gradation distributions. The kurtosis and skewness of color gradient distributions showed the strongest sensitivity to cold stress. Daily minimum temperature was significantly correlated with kurtosis values for R (0.661), G (0.744), B (0.694), and grayscale (0.744) channels. Models relating these parameters to meteorological factors were developed, with polynomial functions outperforming multilinear approaches. All models demonstrated satisfactory fit, as evidenced by determination coefficients exceeding 0.480. The kurtosis model for green values achieved exceptional prediction accuracy, surpassing 90%. Findings demonstrate quantifiable cold-induced changes in canopy color gradient distribution, establishing a foundation for enhancing freeze damage monitoring systems through image-based metrics. These models enable efficient early warning by linking meteorological data to visible canopy responses, offering practical tools for mitigating agricultural cold stress impacts.

DOI: 10.15376/biores.20.3.7162-7178

Keywords: Wheat; Cold spell; Digital images; Color gradation skewed distribution parameters; Response models; Wheat freeze damage warning

*Contact information: a: Key Laboratory for Meteorological Disaster Prevention and Mitigation of Shandong, Jinan 250031; China; b: Shandong Climate Center, Jinan 250031, China; c: Yancheng Meteorological Bureau, Yancheng 224001, China; d: Jiangsu Meteorological Bureau, Nanjing 210008, China; e: Zibo Meteorological Bureau, Zibo 255048, China; f: Key Laboratory of Crop Physiology and Ecology in Southern China, Ministry of Agriculture, Jiangsu Collaborative Innovation Center for Modern Crop Production, National Engineering and Technology Center for Information Agriculture, Nanjing Agricultural University, Nanjing 210095, China; *Corresponding author: 13770068895@163.com*

INTRODUCTION

Global climate change has significantly increased the frequency and intensity of extreme weather events, including unseasonably cold temperature episodes, which pose a significant challenge to agricultural production (Gaupp *et al.* 2020; Benitez-Alfonso *et al.* 2023; Hielkema *et al.* 2023). Wheat, one of the most important sources of human food, is not exempt from these effects. In particular, cold spells, which constitute one of the more commonly observed extreme weather phenomena, can damage the cell structure of wheat plants and cause serious yield losses (Zhu *et al*. 2014). Currently deployed methods aimed at monitoring the severity of low temperature stress exerted on wheat crops mainly rely on manual field observations and sampling, and because this involves expending significant

amounts of time and manpower, their suitability for large-scale applications is limited (Kobayashi *et al*. 2001). In the field of agricultural research, remote sensing technology is increasingly being considered as an economically efficient alternative to traditional analysis methods (Battude *et al*. 2016; Jin *et al*. 2022). However, the spatial and temporal resolution of data obtained from optical satellites rarely meets the criteria that would be required for wheat freeze damage monitoring. In addition, satellite images are highly susceptible to interference by ubiquitous weather phenomena such as clouds, fog, and rain (Yi *et al*. 2024). In essence, both traditional ground surveys and modern satellite-based remote sensing technologies fall short of being able to provide sufficient data enabling the real-time monitoring of wheat freeze damage severity. In order to find an effective approach for the development of an early warning system against wheat freeze damage, the primary challenge is to find an efficient, accurate, and reliable method for characterizing how key wheat growth factors are affected by exposure to cold spells.

There are several alternatives to satellite imaging, including the use of portable imaging devices such as mast or drone-mounted digital cameras. The availability, affordability, and flexibility of these devices have made it increasingly feasible to obtain RGB, multispectral, hyperspectral, light intensity, and thermal data, thus paving the way for non-destructively obtaining color-related information about crop canopies for use in agricultural research. Digital color images are able to record spectral information about a canopy in the visible light band, thereby effectively characterizing the external phenotypic features of the targeted crop. Furthermore, digital color images are able to provide a high level of detail with regard to plant morphology and structure (Zhang *et al*. 2014), which allows researchers to readily extract plant leaf color information from them.

Digital color images are typically encoded using the RGB color space model, which codes each image pixel as a combination of color values for the primary colors red (R), green (G), and blue (B). Beyond these individual color channels, the RGB system also enables the derivation of other color representations, such as the grayscale value. Grayscale, often denoted as 'Y', is a single channel that expresses the brightness of a pixel, devoid of any chromatic information. (Pettorelli *et al*. 2005; Hu *et al*. 2010; Guendouz *et al*. 2012). Examples of research applications of the RGB information contained in digital canopy images include studies on the nitrogen content of winter wheat, the chlorophyll content of rice leaves and the growth process of mangroves (Saberioon *et al*. 2014; Fu *et al*. 2020; Chen *et al*. 2022). So far, however, few studies have investigated how the color of wheat canopies responds to exposure to meteorological elements such as cold spells.

Traditional applications of the RGB model in agricultural research mainly focused on mean color values, thereby largely ignoring any presence of skewness. In their latest research, Zhang *et al*. (2022, 2023) proposed a new way to use the RGB color model by suggesting that the skewness distribution parameters extracted from digital color images of crop canopies might be used to assess the internal physiological status of plants after being exposed to meteorological phenomena. Leveraging this idea makes it possible to incorporate meteorological factors into crop growth models, which would greatly increase their ability to predict potential crop damage. The proposed method relies on a total of 20 so-called Color Gradation Skewed-Distribution (CGSD) parameters extracted from the RGB color information, which includes the mean, median, mode, skewness, and kurtosis associated with the distribution of the color and grayscale values. Specifically, the mean, median, and mode values represent the lightness of the leaf color, while the skewness and kurtosis values represent how the leaf colors are distributed across the color spectrum. Due to their ability to provide an accurate description of different aspects of leaf colors, the CGSD analysis of crop

images has the potential for making a significant contribution to developments in smart agriculture. Although existing research has achieved certain progress in the analysis of the relationship between plant canopy color and meteorology, the model construction in current studies is relatively simple. In addition, the relationship between canopy color and cold waves has not been thoroughly explored. To fill this gap, this study is based on the CGSD parameters of wheat canopy images in Shandong Province for in-depth exploration. It aims to accurately predict the response of wheat canopy to the impact of cold waves and shows higher accuracy and applicability.

The main objectives of this study were to (1) confirm whether cold spells affect the color information in digital images of wheat canopies; (2) investigate the correlation between the CGSD parameters extracted from digital wheat canopy images and a number of key meteorological factors associated with cold spells; and (3) quantify the extent to which the CGSD parameters extracted from digital wheat canopy images respond to exposure cold spells. This research not only enhances the understanding of the relationship between wheat canopy color changes and cold stress but also provides practical tools for mitigating agricultural cold stress impacts.

EXPERIMENTAL

Study Area and Experimental Sites

Located on the eastern coast of China (Fig. 1a), Shandong Province is the pioneering province to achieve a monumental gross agricultural output value exceeding one trillion yuan in China. Qihe county, in the northwestern part of Shandong Province, and the location of the second site was Juxian county, in the southeastern part of Shandong Province (Fig. 1b). Figures 1c-d displayed the photos of these two stations. The selection of experimental sites in northern and southern Shandong can better represent the wheat growth conditions across the province, providing a more comprehensive understanding of the response of wheat canopies to cold spells in different environments (Dong *et al*. 2017).

The experimental subjects were the wheat variety Jimai 22 at the Qihe site and Jimai 44 at the Juxian site. At both sites, the experimental wheat was sowed using strip sowing with a row spacing of 0.2 m. Local differences between the growing environments in the northern and eastern regions of Shandong affected the start of the wheat growing season, which is why the sowing date for the Qihe site (17 October 2022) was earlier than that used for the Juxian site (23 October 2022).

Experimental Design

The experiment was designed to determine the relationship between meteorological factors and CGSD parameters extracted from digital wheat canopy images acquired at two experimental sites over the duration of the 2022-2023 winter wheat growing season. First, digital images of the wheat canopy and local meteorological data were collected from two experimental sites located in Shandong Province, China. The images were grouped and the CGSD parameters were extracted. The modeling samples were subjected to a Pearson correlation analysis. Using the ordinary least squares (OLS) quadratic curve fitting algorithm, a response model between meteorological factors and CGSD parameters was constructed. In order to improve the goodness of fit of the model, a quadratic term was introduced to optimize the initial multiple linear model. Finally, the predictive accuracy of the optimized model was validated by comparing predicted values against actual measurements from both validation and test groups.

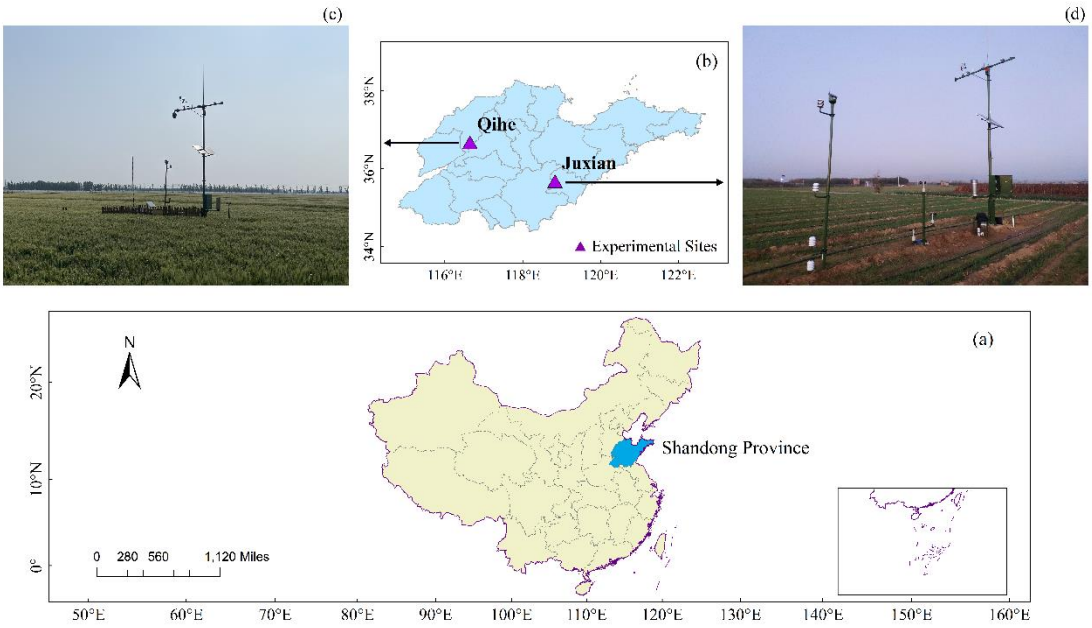

Fig. 1. (a) Location of Shandong Province in China. (b) Distribution of two experimental sites in Shandong Province. (c) A field photograph of the Qihe. Site. (d) A field photograph of the Juxian site

Wheat Canopy Images

The wheat canopy images were acquired *in situ*, using a camera with an image resolution of 1920×1080 pixels (model number: DH-SD-65F630U-HN-Q; manufacturer: Zhejiang Dahua Technology Co. Ltd, China). This camera was mounted at the top of a mast measuring 580 cm in height, installed by the Shandong Meteorological Bureau. When creating the images, a fixed focal length exposure and the automatic white balance feature were provided by the camera. Images were acquired every day at 16:00 for the duration of the experiment. At the Qihe site, the experiment ran from November 23, 2022 to January 26, 2023; and at the Juxian site it ran from November 6, 2022 to January 31, 2023.

To improve the accuracy of the color gradation analysis, images acquired during conditions of intense lighting, frost, or snow cover were discarded, leaving a total of 52 canopy images deemed usable as input for analysis; 31 images were acquired at the Qihe site and 21 images were acquired at the Juxian site. This filtering process resulted in a limited number of images. In order to increase the amount of data and better train and validate the model, samples were constructed by dividing the wheat canopy image into four equal parts, as shown in Fig. 2. It should be noted that the image preprocessing procedure followed Chen *et al*.'s (2020) method to remove soil backgrounds. The upper-left quadrant of each of the 31 images acquired at the Qihe site were designated as modeling samples to be used for regression analysis and model construction, and the three remaining quadrants as samples to be used for model validation (Fig. 2a), providing a total of 31 modeling samples and 93 samples for validation against images from the same site providing the images used for modeling. All four quadrants of the images acquired at the Juxian site were designated to be used for application test (Fig. 2b), providing a total of 84 samples used for validation against results from a different site to the one providing the images used for modeling.

(a)

(b)

Fig. 2. (a) Sample construction from the wheat canopy images acquired at the Qihe site; (b) Sample construction from the wheat canopy images acquired at the Juxian site

Meteorological Data

The experiment used meteorological data collected by in-situ microclimate observatories at each site, as well as national weather stations in Qihe and Juxian. To comprehensively characterize the low-temperature processes and their intensities, this study systematically summarized data on 31 pertinent meteorological factors, as illustrated in Table 1. The foundational data were sourced from Shandong Meteorological Bureau.

Table 1. Meteorological Factors

Factor code	Description
Z1	Effective accumulated temperature since sowing
Z2	Daily mean temperature
Z3	3-day moving average of daily mean temperature
Z4	5-day moving average of daily mean temperature
Z5	Daily mean temperature at 30 cm in wheat fields
Z6	3-day moving average of daily mean temperature at 30 cm in wheat fields
Z7	5-day moving average of daily mean temperature at 30 cm in wheat fields
Z8	Daily mean temperature at 60 cm in wheat fields
Z9	3-day moving average of daily mean temperature at 60 cm in wheat fields
Z10	5-day moving average of daily mean temperature at 60 cm in wheat fields
Z11	Daily mean temperature at 150 cm in wheat fields
Z12	3-day moving average of daily mean temperature at 150 cm in wheat fields
Z13	5-day moving average of daily mean temperature at 150 cm in wheat fields
Z14	Daily minimum temperature
Z15	3-day moving average of daily minimum temperature
Z16	5-day moving average of daily minimum temperature
Z17	24-hour temperature change
Z18	3-day moving average of 24-hour temperature change
Z19	5-day moving average of 24-hour temperature change
Z20	Daily mean dew point temperature
Z21	3-day moving average of daily mean dew point temperature
Z22	5-day moving average of daily mean dew point temperature
Z23	Daily mean grass temperature
Z24	3-day moving average of daily mean grass temperature
Z25	5-day moving average of daily mean grass temperature
Z26	Daily mean relative humidity
Z27	3-day moving average of daily mean relative humidity
Z28	5-day moving average of daily mean relative humidity
Z29	Daily precipitation
Z30	3-day moving average of daily precipitation
Z31	5-day moving average of daily precipitation

Determination of the CGSD Parameters

To determine the CGSD parameters characterizing wheat freeze injury severity, the method proposed by Chen *et al*. (2020) was used. This method involves obtaining a histogram of the cumulative color gradation from the canopy images, and separating, denoising, and ordering the resulting RGB and grayscale information. Prior to the extraction of the CGSD parameters, a normality test was conducted on the collected RGB color data to determine the characteristics of the data distribution. The Jarque-Bera test was used to assess the normality of the pixel value distribution for each color channel (Bera *et al*. 1981). The test results showed that the data of all color channels did not meet the assumption of normal distribution ($p < 0.05$). Then, the mean, median, mode, skewness, and kurtosis functions were used to analyze the canopy leaf CGSD characteristics, respectively. Twenty CGSD parameters were then obtained, including R_{Mean}, R_{Median}, R_{Mode}, R_{Skewness}, R_{Kurtosis}, G_{Mean}, G_{Median}, G_{Mode}, G_{Skewness}, G_{Kurtosis}, B_{Mean}, B_{Median}, B_{Mode}, B_{Skewness}, B_{Kurtosis}, Y_{Mean}, Y_{Median}, Y_{Mode}, Y_{Skewness} and Y_{Kurtosis}.

Construction and Validation of Response Model

The model performance was assessed using key statistical indicators: R-squared, adjusted R-squared, *RMSE* (Root Mean Square Error), and the F-statistic with its significance

level. R-squared measures the model's ability to explain the variance of the dependent variable, with a higher value indicating a better fit to the data. Adjusted R-squared further incorporates a penalty for model complexity by accounting for the number of predictors, where a higher value reflects better model performance after penalizing redundant variables. A smaller RMSE (Root Mean Square Error) signifies lower prediction errors in the model. A larger F-value indicates that at least one predictor variable has a statistically significant impact on the response variable. Notably, a statistically significant model fit was confirmed when the F-statistic's p-value was less than 0.05, adhering to conventional thresholds in hypothesis testing. To evaluate the model, calculate its accuracy based on the following equation (Zhang *et al*. 2023).

$$\mathrm{PA} = \left(1 - \left|\frac{\mathrm{y}_p - y}{y}\right|\right) \times 100\% \quad (1)$$

where projected data are denoted as y_p and actual data are denoted as y.

RESULTS

Impact of Cold Spells on the Color Gradient Distribution in Wheat Canopy Images

The frequency distributions of the R, G, B, and Y values of the pixels extracted from the wheat canopy images acquired at the Qihe site before, during, and after a cold spell are shown in Fig. 3. The time the three images were captured was as close together as possible in order to avoid color differences caused by crop growth. The color gradient distribution curves were slightly shifted to the left over the duration of the cold spell, with the R channel being most strongly affected. Interestingly the curves representing all four values remained being shifted to the left after the cold spell ended, and that their shapes had flattened compared to those representing the times before and during the cold spell. This finding confirms that drastic changes in meteorological conditions can give rise to physiological and biochemical responses in plants that are reflected in the visible light spectrum of crop canopy images (Gitelson *et al*. 2003). In particular, severely adverse conditions caused by climate change can cause crops to exhibit obvious signs of aging, which are typically associated with color changes in the canopy (Han *et al*. 2019). It is therefore no surprise that our results indicate that after a period of exposure to low-temperature stress wheat canopy images exhibit changes with respect to their color gradient distribution.

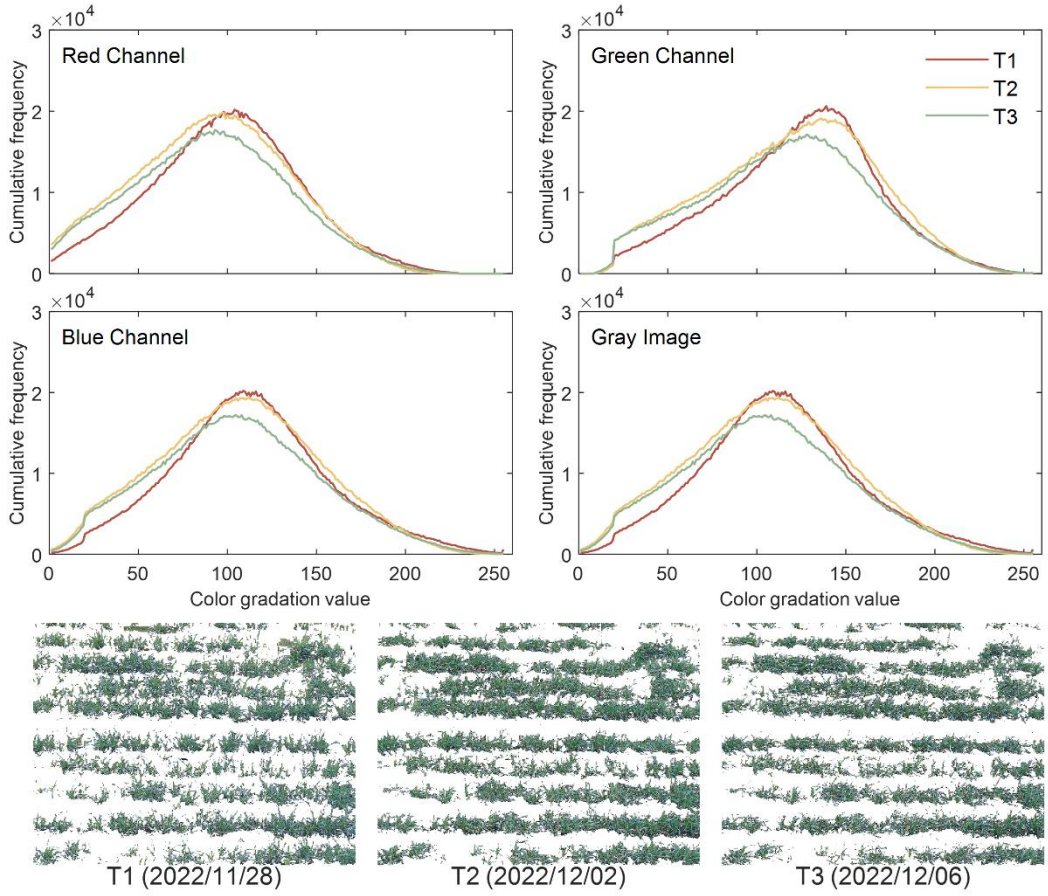

Fig. 3. Frequency distribution of the R, G, B and Y channel of the pixels from wheat canopy image samples acquired at the Qihe site before (T1), during (T2) and after (T3) a cold spell

Correlation between Meteorological Factors and CGSD Parameters

Figure 4 shows the results of a correlation analysis of the 20 CGSD parameters extracted from the modeling samples of our experimental wheat canopies against the 31 meteorological factors used to characterize cold spells. The correlation between individual CGSD parameters and the meteorological factors exhibited large variations. The most notable results were that the kurtosis values of all four color values were positively correlated with most meteorological factors (the only exceptions being *Z1* and *Z17-19*) and that most of these correlations were significant. The highest correlation values were observed between the four kurtosis values and meteorological factor *Z14* (daily minimum temperature), which reached values of 0.661, 0.744, 0.694, and 0.744 for R, G, B and Y, respectively. Regarding the skewness value, it was interesting to note that, at $p \leq 0.01$, the only significantly positively correlated meteorological factor with any of the CGSD parameters was *Z1* (effective accumulated temperature since sowing); the corresponding correlation coefficient exceeded the value of 0.6, whereas all other meteorological factors were either negatively or only weakly positively correlated ($p > 0.05$). The analysis confirmed that the kurtosis and skewness values exhibited a stronger response to meteorological factors associated with cold spells than the other CGSD parameters did.

Neither the mean, median, nor mode values of any of the four color channels exhibited a clear response to any of the meteorological factors, with the exception of R_{Mean}, B_{Mean}, and B_{Median}, which were significantly correlated with Z31; G_{Median}, G_{Mode}, and Y_{Mode}, which were

significantly correlated with *Z1*; B_{Mean}, which was significantly correlated with *Z26*; and B_{Mode}, which was significantly correlated with *Z27*. All correlations in the mean, median and mode values, however, were at a lower significance level ($p \leq 0.05$) than those found for the kurtosis and skewness. In conclusion, of all CGSD parameters associated with digital canopy images, the kurtosis and skewness associated with the distribution of the four color channels exhibited the most sensitive response to meteorological factors related to cold spells. Notably, the response of the kurtosis value was strong enough to be used for further analysis of the relationship between CGSD parameters and meteorological factors.

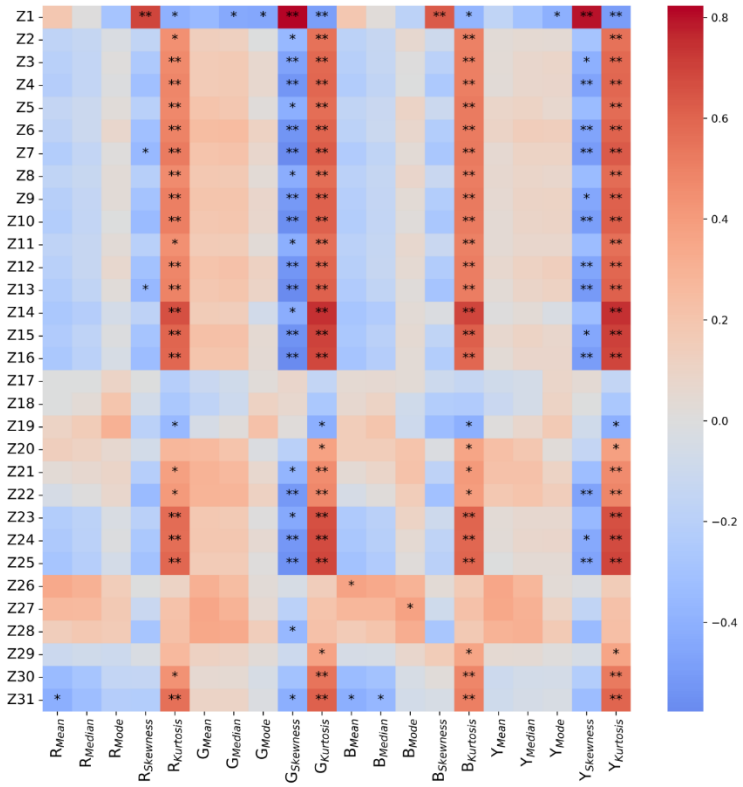

Fig. 4. Heatmap of the correlations between the CGSD parameters extracted from canopy images and meteorological factors associated with cold spells (red for positive, blue for negative). ** indicates a significant correlation at $p \leq 0.01$; * indicates a significant correlation at $p \leq 0.05$.

Construction of the Wheat Canopy Color Response Model

Using the OLS method, each of the CGSD parameters was expressed as a multilinear function of the meteorological factors, after which the goodness of fit of each function was determined (Table 2). In line with an earlier finding that the kurtosis and skewness parameters are significantly correlated with some of the meteorological factors at the 0.01 significance level, the results demonstrated that the goodness of fit of the models representing the response of these parameters was excellent for all four color channels, as indicated by the R-square parameter being greater than or equal to 0.480. Notably, the models for $G_{Skewness}$ and $G_{Kurtosis}$ outperformed all other CGSD parameters, having R-*square* values of 0.677 and 0.742 and *RMSE* scores of 0.150 and 0.368, respectively. It is interesting to note that the main factors that determined the skewness and kurtosis of the image color gradient distribution were *Z1*, *Z5*, and *Z14*. Table 2 also shows that five of the mean, median, and mode parameters could not be modeled (R_{Median}, R_{Mode}, G_{Mean}, Y_{Mean}, and Y_{Median}). The R-square values of the remaining linear models ranged from 0.135 to 0.201, which is significantly worse than the

corresponding values of the skewness and kurtosis parameters, and their adjusted R-square and *RMSE* metrics exhibited the same trend. This result demonstrates that the mean, median, and mode values associated with either the R, G, B and Y channels were not suitable for modeling the response of canopy color to cold spells.

Among the skewness and kurtosis parameters of the four color channels, $G_{Skewness}$ and $G_{Kurtosis}$ exhibited the highest R-square values and the lowest *RMSE* values, indicating that these parameters were the most suitable ones for modeling how the color of wheat canopies responds to meteorological factors.

Table 2. Summary of Modeling Functions and Statistical Metrics for the Relationship Between CGSD Parameters and Meteorological Factors

CGSD parameter	Modeling function	R-square value	Adjusted *R*-square value	*RMSE* value	F value	Significance of *F* value
R_{Mean}	100.192 – 2.990 × Z31	0.167	0.138	6.073	5.818	0.022
$R_{Skewness}$	-3.062 + 0.007 × Z1	0.482	0.465	0.131	27.029	0.000
$R_{Kurtosis}$	3.434 + 0.151 × Z14 – 0.103 × Z5	0.550	0.518	0.315	17.134	0.000
G_{Median}	235.515 – 0.266 × Z1	0.190	0.162	9.582	6.784	0.014
G_{Mode}	370.579 – 0.573 × Z1	0.201	0.173	19.906	7.277	0.000
$G_{Skewness}$	-5.369 + 0.012 × Z1	0.677	0.665	0.150	60.649	0.000
$G_{Kurtosis}$	3.478 + 0.200 × Z14 + 0.296 × Z31 – 0.122 × Z5 + 0.093 × Z18	0.742	0.702	0.368	18.662	0.000
B_{Mean}	113.928 – 3.181 × Z31	0.169	0.140	6.414	5.903	0.022
B_{Median}	111.808 – 2.976 × Z31	0.135	0.106	6.841	4.545	0.042
B_{Mode}	89.511 + 0.230 × Z27	0.144	0.114	7.357	4.872	0.035
$B_{Skewness}$	-3.060 + 0.008 × Z1 + 0.012 × Z14	0.480	0.443	0.127	12.910	0.000
$B_{Kurtosis}$	3.498 + 0.172 × Z14 – 0.111 × Z5	0.578	0.548	0.356	19.175	0.000
Y_{Mode}	293.225 – 0.418 × Z1	0.163	0.134	16.476	5.658	0.024
$Y_{Skewness}$	-4.658 + 0.011 × Z1	0.635	0.622	0.144	50.374	0.000
$Y_{Kurtosis}$	3.646 + 0.212 × Z14 – 0.126 × Z5	0.632	0.606	0.415	24.040	0.000

Optimization of the Wheat Canopy Color Response Model

To optimize the goodness of fit of the functions used to model the CGSD parameters that had performed best during our initial multilinear approach ($G_{Skewness}$ and $G_{Kurtosis}$), quadratic terms were introduced. The resulting polynomial functions outperformed the multilinear functions, as indicated by their R-square values, which reached 0.682 for the quadratic function used to model $G_{Skewness}$ and 0.775 for the quadratic function used to model $G_{Kurtosis}$. When comparing the other indicators for the goodness of fit, both the adjusted R-square and *RMSE* value for the polynomial function used to model $G_{Skewness}$ were marginally worse than the corresponding values for the multilinear model (Fig. 5), but for the function used model $G_{Kurtosis}$ they were both better (Fig. 6). Overall, the goodness of fit of the polynomial functions used to model both $G_{Skewness}$ and $G_{Kurtosis}$ was superior to that of the multilinear functions, which is consistent with previously reported findings that polynomial functions can more effectively model climate responses than multilinear ones (Zhang *et al*. 2023). The polynomial function models have been found to be superior to multilinear methods in capturing the relationship between meteorological factors and wheat canopy color distribution parameters, which is consistent with the research of Zhang et al. (2022). The possible reason is that the duration and intensity of cold stress interact in complex ways to influence plant physiology and, consequently, the canopy color. The polynomial terms in the models allow for a more flexible and accurate representation of these non-linear interactions, thereby improving the model fit and predictive power.

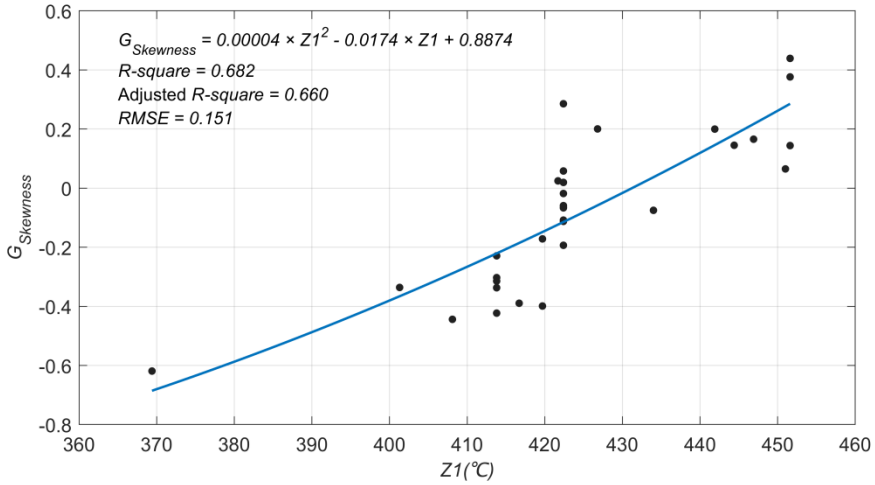

Fig. 5. Optimized polynomial function used to model $G_{Skewness}$

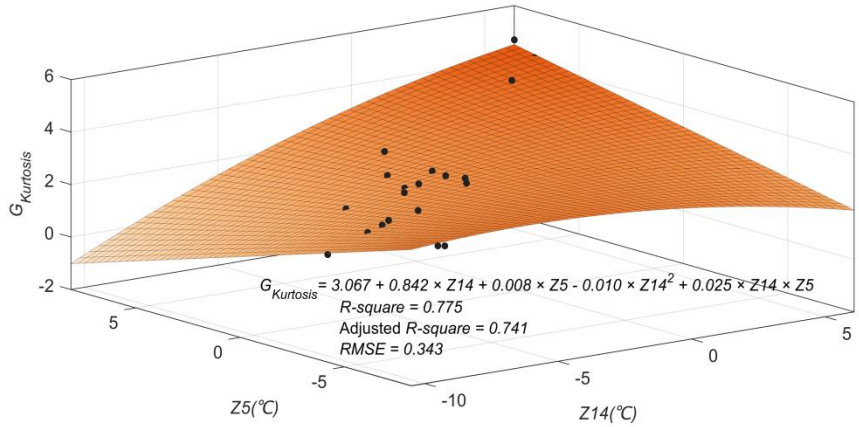

Fig. 6. Optimized polynomial function used to model $G_{Kurtosis}$

Prediction Accuracy of The Optimized $G_{Kurtosis}$ Model

Figure 7 shows violin plots depicting the probability density of the prediction accuracy of the $G_{Kurtosis}$ model with respect to the modeling group used to construct it, the validation group from the same site (Qihe), and the application test group from the other site (Juxian). The plots indicate that the model's prediction accuracy for all three groups types was good: Although there were only 31 modeling samples, the median prediction accuracy with respect to the modeling group reached 93.22%. The prediction accuracy with respect to the validation group and application test group were also excellent, having median values of 89.50% for samples from the site providing the former, 90.01% for samples from the latter. Notably, the shapes of the violin plots for groups taken at modeling and validation were similar, which may be due to the fact that the samples were acquired under consistent climatic conditions. It is also interesting to note that, although the overall prediction accuracy with respect to the application test group was slightly lower than that with respect to the modeling group, the most probable prediction accuracies were still between 85% and 95%. Finally, it should be noted that the probability density decreases slightly near the median prediction accuracy, and that there are no outliers in the prediction accuracy values for any sample type.

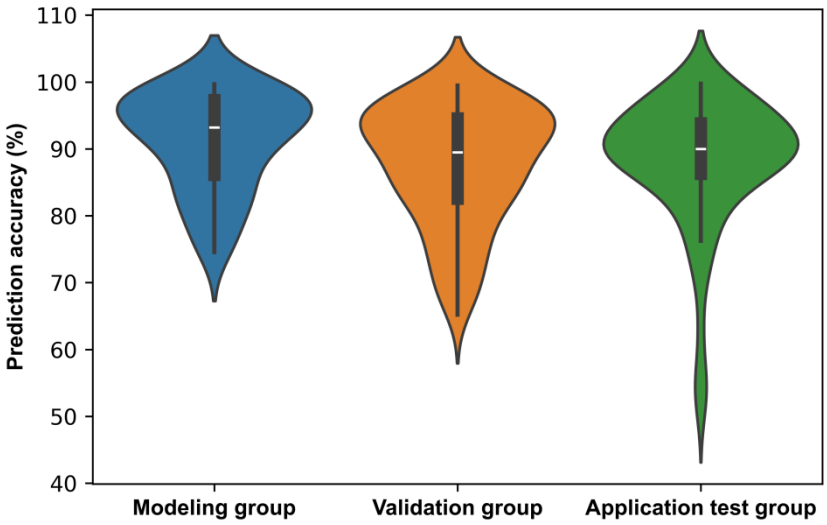

Fig. 7. Violin plots depicting the probability density of the prediction accuracy of the meteorological response model for $G_{Kurtosis}$ for the different sample types included in our experiment

DISCUSSION

Previous studies have shown that crop leaves can play a crucial role in generating nutrients (Großkinsky *et al*. 2018), and that their color, as a typical phenotypic feature, reflects the crop's growth status (Vasseur *et al*. 2018). For this reason, it was hypothesized that it must be possible to obtain information about the growth and development of crops exposed to cold spell from digital images using the widely used RGB format. The CGSD features of wheat canopy images were extracted, and the relationship between those features and a number of meteorological factors related to cold spells were studied. In this study, the response model of CGSD parameters to meteorological factors was established for the first time to study the response of wheat crops to cold wave in Shandong Province.

The results exhibited certain differences between the CGSD parameters extracted from wheat canopy images captured at the same location but at different times. A possible explanation is the fact that the digital cameras automatically adjust their exposure time and image calibration parameters to the ambient lighting conditions (Muñoz-Huerta *et al*. 2013; Barbedo *et al*. 2016; Wang *et al*. 2016). Growth and development of wheat may also lead to changes in image data. Nevertheless, the present findings exhibited uncontroversial evidence of the RBG values and color gradient distribution of the pixels making up wheat canopy images being affected by exposure to cold spells (Bera *et al*. 1981).

Although the color gradient distribution of RGB images of plant leaves typically exhibits a certain amount of skewness (Bera *et al*. 1981; Chen *et al*. 2020), existing research has tended to overlook skewness, mainly focusing on analyzing the mean and standard deviation of the color gradient distribution. The 20 CGSD parameters used in this study greatly expanded the number of color gradient distribution parameters extracted from the digital images and allowed a more rational and systematic characterization of the leaf colors. The findings indicated that the mean, mode, and median values associated with the color gradient distribution correlated only weakly with the meteorological factors related to cold spells, while the skewness and kurtosis correlate strongly. This may be due to the physiological processes of wheat plants being affected when they encounter cold waves,

leading to changes in plant pigments and cell structure. The skewness of the color distribution reflects the asymmetry of color changes across different parts of the canopy, while the kurtosis indicates the degree of color concentration or dispersion (Zhang *et al.* 2022, 2023). These changes in skewness and kurtosis can be effectively captured by digital image analysis, making them sensitive indicators of cold stress. For this reason, this study prioritized the use of skewness and kurtosis as the key parameters for polynomial modeling how the color gradient distribution of wheat canopy images responds to cold spells. This study showed the feasibility of using CGSD parameters to construct accurate and stable models for how the color gradient distribution of digital wheat canopy images respond to meteorological factors related to cold spells.

Overall, the research results indicated that skewness and kurtosis parameters were the most sensitive to cold stress, demonstrating the potential of using color parameters to reflect plant stress and emphasizing the importance of color distribution in understanding plant physiological states. Moreover, the polynomial functions provided a better fit to the data, which can more effectively capture the non-linear responses of wheat canopy color to cold stress. This suggests that the relationship between canopy color and cold stress is inherently non-linear. These results are consistent with previous research findings (Zhang *et al.* 2023 and Chen *et al.* 2020). The constructed response model of wheat canopy color to cold spells holds significant promise for cold wave warning systems. It enables the prediction of potential cold damage by monitoring changes in canopy color, which are indicative of plant stress. This can help agricultural authorities and farmers to take proactive measures to reduce the risk of yield losses.

Future work is needed to collect more data and involve advanced modeling methods such as deep learning and machine. To expand the scope of this results, the relationship between meteorological factors and the color gradient distribution of wheat canopy images potentially involves many spectral features not captured by the CGSD parameters, such as the green leaf vegetation index (GLI) (Hunt *et al*. 2011), the modified green red vegetation index (MGRVI) (Bendig *et al*. 2015), the visual atmospheric resistance vegetation index (VARI) (Gitelson *et al*. 2022), and the excess red vegetation index (ExR) (Mao *et al*. 2004), as well as several other color and texture features such as HSV, Lab, Lch, Luv, (Cheng *et al*. 2001; García-Mateos *et al*. 2015; Viscarra *et al*. 2006), angular second moment (ASM), contrast (CON), correlation (COR), and entropy (ENT) (Haralick *et al*. 1973). Finally, it might be worth analyzing the response relationship between CGSD parameters and other crop-related factors, such as meteorological factors in terms of growth stage (Großkinsky *et al*. 2018), soil quality, or even latitude and longitude.

CONCLUSIONS

1. Exposure to low-temperature stress can significantly affect the kurtosis values associated with the color gradient distribution of digital wheat canopy images. The coefficients of determination for the relationships between R_{Kurtosis}, G_{Kurtosis}, B_{Kurtosis} and Y_{Kurtosis} and the daily minimum temperature reached 0.661, 0.744, 0.694, and 0.744, respectively.
2. Both the skewness and kurtosis of the RGB color and grayscale value distribution of pixels from wheat canopy images could be accurately modeled. All models featuredba an R-square coefficient that exceeded the value of 0.480.
3. The goodness of fit of the optimized models was good. The polynomial models for

$G_{Skewness}$ and $G_{Kurtosis}$ featured adjusted R-square values of 0.660 and 0.741, respectively, which was even better than the corresponding values we obtained for the multilinear models.

4. The prediction accuracy of the polynomial $G_{Kurtosis}$ curve model was excellent, reaching 93.22%, 89.50%, and 90.01% with respect to the modeling group, validation group, and application test group, respectively.

ACKNOWLEDGEMENTS

This research was supported by the Science and Technology Project of Jiangsu Meteorological Bureau (KM202303) and the key project of science and technology research of Shandong Meteorological Bureau (2023sdqxzl2). All methods and data in this study were carried out in accordance with relevant guidelines and regulations. The authors are grateful to the Shandong Meteorological Bureau for providing digital wheat canopy images and meteorological data.

Author Contributions

Jibo Zhang: Designed experiments and wrote manuscript. Hongwei Zhou: Methodology, Writing – review and editing. Chuanxiang Yi: Methodology, Writing – original draft, Writing – review and editing. Pei Zhang: Methodology, Writing – review and editing. Haijun Huan and Feifei Xu: Formal analysis. Qi Chen and Qiqing Shan: Investigation. Ye Sheng and Qin Mei: Formal analysis. All authors read and approved the final manuscript.

Competing Interests

The authors declare no competing interests.

Data Availability

The datasets used and analyzed during the current study available from the corresponding author on reasonable request.

REFERENCES CITED

Barbedo, J. G. A. (2016). "A review on the main challenges in automatic plant disease identification based on visible range images," *Biosystems Engineering* 144, 52-60. DOI: 10.1016/j.biosystemseng.2016.01.017

Battude, M., Al Bitar, A., Morin, D., Cros, J., Huc, M., Marais Sicre, C., Le Dantec, V., and Demarez, V. (2016). "Estimating maize biomass and yield over large areas using high spatial and temporal resolution Sentinel-2 like remote sensing data," *Remote Sensing of Environment* 184, 668-681. DOI: 10.1016/j.rse.2016.07.030.

Bendig, J., Yu, K., Aasen, H., Bolten, A., Bennertz, S., Broscheit, J., Gnyp, M.L., and Bareth, G. (2015). "Combining UAV-based plant height from crop surface models, visible, and near infrared vegetation indices for biomass monitoring in barley," *International Journal of Applied Earth Observation and Geoinformation* 39, 79-87. DOI: 10.1016/j.jag.2015.02.012

Benitez-Alfonso, Y., Soanes, B. K., Zimba, S., Sinanaj, B., German, L., Sharma, V., Bohra,

A., Kolesnikova, A., Dunn, J. A., Martin, A. C., *et al*. (2023). "Enhancing climate change resilience in agricultural crops," *Current Biology* 23, article 33. DOI: 10.1016/j.cub.2023.10.028

Bera, A. K., and Jarque, C. M. (1981). "Efficient tests for normality, homoscedasticity and serial independence of regression residuals: Monte Carlo evidence," *Economics Letters* 7, 313-318. DOI: 10.1016/0165-1765 (81) 90035-5

Chen, Y., Fang, S., Sun, M., Liu, Z., Pan, L., Mo, W., and Chen, C. (2022). "Mangrove growth monitoring based on camera visible images—A case study on typical mangroves in Guangxi," *Frontiers in Earth Science* 9, article 771753. DOI: 10.3389/feart.2021.771753.

Chen, Z., Wang, F., Zhang, P., Ke, C., Zhu, Y., Cao, W., and Jiang, H. (2020). "Skewed distribution of leaf color RGB model and application of skewed parameters in leaf color description model," *Plant Methods* 16, 23. DOI: 10.1186/s13007-020-0561-2

Cheng, H. D., Jiang, X. H., Sun, Y., and Wang, J. (2001). "Color image segmentation: Advances and prospects," *Pattern Recognition* 34, 2259-2281. DOI: 10.1016/S0031-3203(00)00149-7

Fu, Y., Yang, G., Li, Z., Song, X., Li, Z., Xu, X., Wang, P., and Zhao, C. (2020). "Winter wheat nitrogen status estimation using UAV-based RGB imagery and Gaussian processes regression," *Remote Sensing* 12, article 3778. DOI: 10.3390/rs12223778

García-Mateos, G., Hernández-Hernández, J. L., Escarabajal-Henarejos, D., Jaén-Terrones, S., and Molina-Martínez, J. M. (2015). "Study and comparison of color models for automatic image analysis in irrigation management applications," *Agricultural Water Management* 151, 158-166. DOI: 10.1016/j.agwat.2014.08.010

Gaupp, F., Hall, J., Hochrainer-Stigler, S., and Dadson, S. (2020). "Changing risks of simultaneous global breadbasket failure," *Nat. Clim. Chang.* 10, 54-57. DOI: 10.1038/s41558-019-0600-z

Gitelson, A. A., Gritz, Y., and Merzlyak, M. N. (2003). "Relationships between leaf chlorophyll content and spectral reflectance and algorithms for non-destructive chlorophyll assessment in higher plant leaves," *Journal of Plant Physiology* 160, 271-282. DOI: 10.1078/0176-1617-00887

Gitelson, A. A., Stark, R., Grits, U., Rundquist, D., Kaufman, Y., and Derry, D. (2022). "Vegetation and soil lines in visible spectral space: A concept and technique for remote estimation of vegetation fraction," *International Journal of Remote Sensing* 23, 2537-2562. DOI: 10.1080/01431160110107806

Großkinsky, D. K., Syaifullah, S. J., and Roitsch, T. (2018). "Integration of multi-omics techniques and physiological phenotyping within a holistic phenomics approach to study senescence in model and crop plants," *Journal of Experimental Botany* 69, 825-844. DOI: 10.1093/jxb/erx333.

Guendouz, A., Guessoum, S., Maamari, K., and Hafsi, M. (2012). "Predicting the efficiency of using the RGB (red, green and blue) reflectance for estimating leaf chlorophyll content of durum wheat (*Triticum durum* Desf.) genotypes under semi arid conditions," *American-Eurasian Journal of Sustainable Agriculture* 102-107.

Han, W., Yang, Z., Huang, L., Sun, C., Yu, X., and Zhao, M. (2019). "Fuzzy comprehensive evaluation of the effects of relative air humidity on the morpho-physiological traits of pakchoi (*Brassica chinensis* L.) under high temperature," *Scientia Horticulturae* 246, 971-978. DOI: 10.1016/j.scienta.2018.11.079

Haralick, R. M., Shanmugam, K., and Dinstein, I. (1973). "Textural features for image classification," *IEEE Transactions on Systems, Man, and Cybernetics* SMC-3, 610-621.

DOI: 10.1109/TSMC.1973.4309314.

Hielkema, T.W., Schipper, C.A., and Gersonius, B. (2023). "Global nature conservation and the apparent ineffective adaptation to climate pressures," *Aquatic Ecosystem Health and Management* 26, 33-46. DOI: 10.14321/aehm.026.02.033.

Hu, H., Liu, H., Zhang, H., Zhu, J., Yao, X., Zhang, X., Zheng, K. (2010). "Assessment of chlorophyll content based on image color analysis, comparison with SPAD-502," in: *2010 2nd International Conference on Information Engineering and Computer Science*, Wuhan, China. DOI: 10.1109/ICIECS.2010.5678413

Hunt Jr., E. R., Daughtry, C. S. T., Eitel, J. U. H., and Long, D. S. (2011). "Remote sensing leaf chlorophyll content using a visible band index," *Agronomy Journal* 103, 1090-1099. DOI: 10.2134/agronj2010.0395

Jin, N., Tao, B., Ren, W., He, L., Zhang, D., Wang, D., and Yu, Q. (2022). "Assimilating remote sensing data into a crop model improves winter wheat yield estimation based on regional irrigation data," *Agricultural Water Management* 266, article 107583. DOI: 10.1016/j.agwat.2022.107583

Kobayashi., Kanda., Kitada., *et al*. (2001). "Detection of rice panicle blast with multispectral radiometer and the potential of using airborne multispectral scanners," *Phytopathology* 91(3), 316-23. DOI: 10.1094/PHYTO.2001.91.3.316

Mao, D., Wu, X., Deppong, C., Friend, L. D., Dolecki, G., Nelson, D. M., and Molina, H. (2004). "Negligible role of antibodies and C5 in pregnancy loss associated exclusively with C3-dependent mechanisms through complement alternative pathway," *Immunity* 19, 813-822. DOI: 10.1016/S1074-7613(03)00321-2

Muñoz-Huerta, R. F., Guevara-Gonzalez, R. G., Contreras-Medina, L. M., Torres-Pacheco, I., Prado-Olivarez, J., and Ocampo-Velazquez, R. V. (2013). "A review of methods for sensing the nitrogen status in plants: Advantages, disadvantages and recent advances," *Sensors* 13, 10823-10843. DOI: 10.3390/s130810823

Pettorelli, N., Vik, J. O., Mysterud, A., Gaillard, J.-M., Tucker, C. J., and Stenseth, N. Chr. (2005). "Using the satellite-derived NDVI to assess ecological responses to environmental change," *Trends in Ecology & Evolution* 20, 503-510. DOI: 10.1016/j.tree.2005.11.006

Saberioon, M. M., Amin, M. S. M., Anuar, A. R., Gholizadeh, A., Wayayok, A., and Khairunniza-Bejo, S. (2014). "Assessment of rice leaf chlorophyll content using visible bands at different growth stages at both the leaf and canopy scale," *International Journal of Applied Earth Observation and Geoinformation* 32, 35-45. DOI: 10.1016/j.jag.2014.03.018

Vasseur, F., Bresson, J., Wang, G., Schwab, R., and Weigel, D. (2018). "Image-based methods for phenotyping growth dynamics and fitness components in *Arabidopsis thaliana*," *Plant Methods* 14, article 63. DOI: 10.1186/s13007-018-0331-6.

Viscarra Rossel, R. A., Minasny, B., Roudier, P., and McBratney, A. B. (2006). "Colour space models for soil science," *Geoderma* 133, 320-337. DOI: 10.1016/j.geoderma.2005.07.017.

Wang, C., Guo, X., Wen, W., Du, J., and Xiao, B. (2016). "Application of hemispherical photography on analysis of maize canopy structural parameters under natural light," *Transactions of the Chinese Society of Agricultural Engineering* 32, 157-162. DOI: 10.11975/j.issn.1002-6819.2016.04.022.

Yi, C., Li, X., Xing, Z., Xin, X., Ren, Y., Zhou, H., Zhou, W., Zhang, P., Wu, T., and Wigneron, J.-P. (2024). "An assessment of the seasonal uncertainty of microwave L-band satellite soil moisture products in Jiangsu Province," *China. Remote Sens.* 16,

article 4235. DOI: 10.3390/rs16224235.

Zhang, Y. H., Liang, Q. T., Liu, X. J., Liu, L. L., Can, W. X, and Zhu, Y. (2014). "Modeling dynamics of leaf color based on RGB value in rice," *Journal of Integrative Agriculture* 13, 749-759. DOI: 10.1016/S2095-3119(13)60391-3.

Zhang, P., Chen, Z., Wang, F., Wang, R., Bao, T., Xie, X., An, Z., Jian, X., and Liu, C. (2022). "Response of population canopy color gradation skewed distribution parameters of the RGB model to micrometeorology environment in *Begonia fimbristipula* Hance," *Atmosphere* 13, article 890. DOI: 10.21203/rs.3.rs-319948/v1

Zhang, P., Chen, Z., Wang, F., Wu, H., Hao, L., Jiang, X., Yu, Z., Zou, L., and Jiang, H. (2023). "Response and inversion of skewness parameters to meteorological factors based on RGB model of leaf color digital image," *PLOS ONE* 18, article e0288818. DOI: 10.1371/journal.pone.0288818

Zhu, J., Pearce, S., Burke, A., See, D. R., Skinner, D. Z., Dubcovsky, J., and Garland-Campbell, K. (2014). "Copy number and haplotype variation at the VRN-A1 and central FR-A2 loci are associated with frost tolerance in hexaploid wheat," *Theor. Appl. Genet.* 127, 1183-1197. DOI: 10.1007/s00122-014-2290-2.

Article submitted: April 9, 2025; Peer review completed: June 1, 2025: Revisions accepted: June 25, 2025. Published: July 10, 2025.
DOI: 10.15376/biores.20.3.7162-7178